Reactive & Functional Polymers 69 (2009) 530–538

Contents lists available at ScienceDirect

Reactive & Functional Polymers

journal homepage: www.elsevier.com/locate/react

Self-assembling behavior of block copolymers involving competing length scales

Ching-I Huang *

Institute of Polymer Science and Engineering, National Taiwan University, Taipei 106, Taiwan

ARTICLE INFO

Article history:
Available online 27 January 2009

Keywords:
Block copolymer
Self-assembling
Hierarchical structure
Structure-within-structure
Dissipative particle dynamics

ABSTRACT

This paper highlights our recent results concerning the self-assembling behavior of block copolymers, in which two length-scale-ordering morphologies are involved, by employing the dissipative particle dynamics (DPD) method. In particular, two molecular architectures by combining an A-homopolymer block with a BC-comb block or a BC-alternating block, which are referred as A-*block*-(B-*graft*-C) and A_2-*star*-(B-*alt*-C), respectively, are examined. Generally speaking, as long as the three components are significantly incompatible one another, various types of hierarchical structures, such as spheres-within-lamellae, cylinders-within-lamellae, gyroid-within-lamellae, lamellae-within-lamellae, lamellae-within-cylinders, and lamellae-within-spheres, can be formed in both molecular architectures. However, they exhibit a completely different packing behavior of molecules due to the difference of molecular architecture. In particular, the small-length-scale lamellae formed by the B-*alt*-C and B-*graft*-C chains display a parallel and perpendicular direction, respectively, with respect to the large-length-scale structure. We believe this characteristic difference could impose different influences upon various properties of polymers, such as photoelectronic properties, and lead to different potential applications.

1. Introduction

Due to its variant self-assembling behavior, block copolymers are widely applied in many nanotechnologies, such as photonic and biotechnological applications [1,2]. Generally speaking, traditional AB linear diblock copolymers form microphase-separated structures at only one characteristic length scale usually within 10–100 nm range, when the incompatibility degree between A and B is significant. Recently, with the improvement in synthetic techniques, copolymers with more complex architectures or more than two types of monomers have been successfully formulated. This development leads to a rich variety of more fantastic morphologies at multiple length scales. The unique character of hierarchical structures implies brand-new material properties and thus offers possibilities for block copolymers towards novel technologies and applications [3–6].

To create additional length-scale-ordering within the microphase-separated domains, most of the research has mainly adopted the supramolecular chemistry concept to synthesize the A-*block*-(B-*graft*-C) coil-comb copolymers, in which the component C is typically a short chain molecule and grafted to the backbone B through the noncovalent bonding interactions [3–13]. In this case, various types of structure-within-structures, such as spheres-within-lamellae, cylinders-within-lamellae, gyroid-within-lamellae, lamellae-within-lamellae, lamellae-within-cylinders, and lamellae-within-spheres, can form upon varying the block composition. The large-length-scale-ordering morphology is mainly driven by the segregation between the A-coil blocks and the BC-comb blocks, and hence depends on the block composition. Once the segregation degree between B and C becomes significantly large, a small-length-scale-ordering of B and C alternating layers with a characteristic size of several nanometers frequently occurs within the original BC-rich domains. For example, Ikkla and ten Brinke and coworkers [3–5,12] synthesized a series of polystyrene-*block*-poly(4-vinylpyridine) (PS-*block*-P4VP) copolymers with pentadecylphenol (PDP) as side chains, which are grafted into the P4VP blocks through hydrogen bonds. The resulting coil-comb copolymers, examined by transmission electron microscopy (TEM) and small angle X-ray scattering (SAXS), display a variety of the above mentioned hierarchical structures with two different length scales at room temperature. Moreover, they observed that further heating leads to a gradually reduced hydrogen bonding strength between P4VP and PDP, and thereafter induces a series of large-length-scale diblock–like morphology transitions. Tsao and Chen [13] also observed the formation of structure-within-structure in poly(1,4-butadiene)-*block*-poly(ethylene oxide) (PB-*block*-PEO) with dodecylbenzenesulfonic acid (DBSA) attached to PEO through hydrogen bonds. In addition, they reported that a large-scale morphology transition can be driven by the small-length-scale transition concurrently in this PB-*block*-(PEO-*graft*-DBSA) copolymers.

In fact, coil-comb copolymers are not the only ones that can self-assemble to form hierarchical structures. By substituting the B-*graft*-C comb block with the B and C alternating block (denoted

* Tel.: +886 2 33665886; fax: +886 2 33665237.
E-mail address: chingih@ntu.edu.tw

1381-5148/$ - see front matter © 2009 Elsevier Ltd. All rights reserved.
doi:10.1016/j.reactfunctpolym.2009.01.010

as B-*alt*-C), it is also possible to generate the small-length-scale structures within the large-scale domains. Experimentally, Matsushita and co-workers first synthesized an undecablock terpolymer of styrene (S)–isoprene (I), in which both S end-blocks are long and the middle S and I alternating blocks are short. They observed the formation of thin S and I alternating lamellae and thick S-formed lamellae [14]. It is worthy to note that the two-length-scale-ordering lamellae formed in this coil-alternating copolymer system are in parallel, which is quite different from those formed perpendicular to each other in comb-coil copolymers. In addition to lamellar-within-lamellar structure, they have recently observed other hierarchical structures, such as spheres-within-lamellae, cylinders-within-lamellae, coaxial cylinders, and cocentric spheres, from the undecablock terpolymer consisting of two long poly(2-vinylpyridine) (P) end-blocks and short S and I alternating middle-blocks [15,16].

As manifested above experimentally, both coil-comb and coil-alternating block copolymers have been shown good candidates to form hierarchical structure-within-structures. A thorough understanding of the resulting self-assembling behavior for these two copolymers thus becomes a very important and interesting topic. A few related theoretical work has been initiated by ten Brinke and co-workers [17–20]. For instance, they analyzed the phase behavior of A-*block*-(A-*graft*-B) coil-comb copolymers in the weak segregation limit, and observed a competing phenomenon of two length-scale-ordering structures [17,18]. When the A-coil block length is short, the formed microstructure is mainly driven by the segregation between the A and B within the comb block; while a diblock-like microphase separation between the A-coil and AB-comb blocks tends to occur when the A-coil is long. Later, they examined the self-assembling behavior of A-*block*-(B-*alt*-A) block copolymers via a reciprocal-space self-consistent mean-field (SCMF) theory [19,20]. Similar to the coil-comb architecture, these A-*block*-(B-*alt*-A) molecules can form the above small-length-scale and large-length-scale microstructures depending on the ratio of coil and alternating block lengths. In addition, if both blocks have comparable lengths, a hierarchical lamellar-within-lamellar structure (i.e., coexistence of two length-scale-ordering lamellae) can be formed. Compared with the experimental studies, one may notice the fact that the current theoretical results by ten Brinke group cannot catch the formation of various types of hierarchical structure-within-structures in either coil-comb or coil-alternating copolymer. This may be due to the fact that only two types of monomers are involved in the currently examined systems. Moreover, though the SCMF technique in reciprocal-space adopted by them is numerically efficient and allows high precision calculations of free energies, the requirement of the basis functions for assumed phase symmetry makes it unsuitable to deal with the more and more complicated morphologies generated by these molecular architectures.

Recently, we thus employ a direct simulation method, known as the dissipative particle dynamics (DPD) simulation technique [21,22], to examine the self-assembling behavior of A-*block*-(B-*graft*-C)) and A_2-*star*-(B-*alt*-C) molecules. To clarify, no assumption of any phase symmetry is needed in this simulation technique. Generally speaking, the DPD method simplifies a long series of molecular groups into a few bead-and-spring type particles, and therefore it can simulate the molecular behavior on longer time-scales and larger length scales compared with the classical molecular dynamics and Monte Carlo simulations. However, compared with the SCMF calculations, the modeled chains are indeed very short, and therefore the associated entropic effects on the resulting phase behavior with long chains may not be reflected appropriately. Hence, the morphological behavior, in particular in the weak segregation regime, may differ when the chain length N increases. When the segregation degree becomes significantly large, so that the formation of well ordered structures is mainly dominated by the enthalpic effects, the self-assembling behavior simulated for short chains via DPD should also hold true qualitatively for long copolymer chains. Accordingly, our results via DPD in these two systems have captured most of the important and interesting hierarchical structure-within-structures observed in the experimental work. This report highlights our recent findings concerning the self-assembling behavior of A-*block*-(B-*graft*-C)) and A_2-*star*-(B-*alt*-C) copolymers, in which two length-scale-ordering morphologies are involved [23,24]. Our modeled chains are illustrated in Fig. 1. It should be mentioned that in simulating the phase behavior associated with the coil-alternating copolymers, we choose the A_2-*star*-(B-*alt*-C) molecules, in which the BC-alternating block is linked to the middle of the A-homopolymer block instead of the end of A-block (referred as A-*block*-(B-*alt*-C)). By doing so, the simulation box and time can be reduced. Though there exists a slight difference of molecular architecture between our simulated A_2-*star*-(B-*alt*-C) and experimental A-*block*-(B-*alt*-C), both results are qualitatively in good agreement. Indeed, this is not surprising by recalling that both A_2B star and AB linear copolymers also exhibit similar morphology patterns [25,26].

2. DPD simulation method

In the DPD simulation [21], the time evolution of motion for a set of interacting particles is solved by Newton's equation. For simplicity, we assume that the masses of all particles are equal to 1. The force acting on the i-th particle $\vec{f}_i$ contains three parts: a conservative force $\vec{F}^{C}_{ij}$, a dissipative force $\vec{F}^{D}_{ij}$, and a random force $\vec{F}^{R}_{ij}$, i.e.,

$$\vec{f}_i = \sum_{i \neq j} (\vec{F}^{C}_{ij} + \vec{F}^{D}_{ij} + \vec{F}^{R}_{ij}) \tag{1}$$

where the sum is over all other particles within a certain cut-off radius r_c. As this short-range cut-off counts only local interactions, r_c is usually set to 1 so that all lengths are measured relative to the particle radius.

The conservative force $\vec{F}^{C}_{ij}$ is a soft repulsive force and given by

$$\vec{F}^{C}_{ij} = \begin{cases} -a_{ij}(1 - \frac{r_{ij}}{r_c})\vec{n}_{ij} & r_{ij} < r_c \\ 0 & r_{ij} \geqslant r_c \end{cases} \tag{2}$$

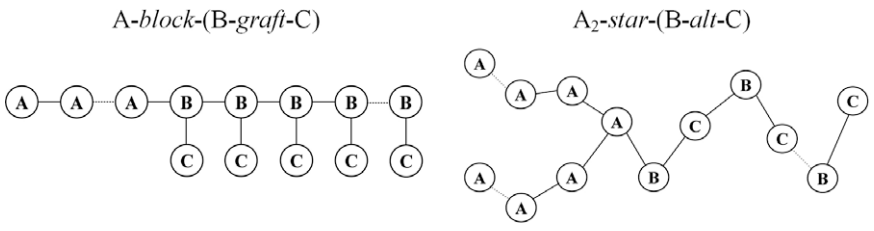

Fig. 1. Schematic plot of our simulated A-*block*-(B-*graft*-C) and A_2-*star*-(B-*alt*-C) molecules.

where a_{ij} is the repulsive interaction parameter between particles i and j, $\vec{r}_{ij} = \vec{r}_j - \vec{r}_i, r_{ij} = |\vec{r}_{ij}|$, and $\vec{n}_{ij} = \frac{\vec{r}_{ij}}{r_{ij}}$.

The dissipative force $\vec{F}_{ij}^{D}$ is a hydrodynamic drag force and given by:

$$\vec{F}_{ij}^{D} = \begin{cases} -\gamma\omega^{D}(r_{ij})(\vec{n}_{ij}\cdot\vec{v}_{ij})\vec{n}_{ij} & r_{ij} < r_c \\ 0 & r_{ij} \geqslant r_c \end{cases} \quad (3)$$

where γ is a friction parameter, ω^{D} is an r-dependent weight function vanishing for $r \geqslant r_c$, and $\vec{v}_{ij} = \vec{v}_j - \vec{v}_i$.

The random force $\vec{F}_{ij}^{R}$ corresponds to the thermal noise and has the form of

$$\vec{F}_{ij}^{R} = \begin{cases} \sigma\omega^{R}(r_{ij})\theta_{ij}\vec{n}_{ij} & r_{ij} < r_c \\ 0 & r_{ij} \geqslant r_c \end{cases} \quad (4)$$

where σ is a parameter, ω^{R} is a weight function, and $\theta_{ij}(t)$ is a randomly fluctuating variable. Note that these two forces $\vec{F}_{ij}^{D}$ and $\vec{F}_{ij}^{R}$ also act along the line of centers and conserve linear and angular momentum. There is an independent random function for each pair of particles. Also there is a relation between both constants γ and σ as follows [22],

$$\sigma^2 = 2\gamma k_B T \quad (5)$$

In our simulations, $\gamma = 4.5$ and the temperature $k_BT = 1$. As such, $\sigma = 3.0$ according to Eq. (5).

In order for the steady-state solution to the equation of motion to be the Gibbs ensemble and for the fluctuation–dissipation theorem to be satisfied, it has been shown that only one of the two weight functions ω^{D} and ω^{R} can be chosen arbitrarily [27],

$$\omega^{D}(r) = [\omega^{R}(r)]^2 \quad (6)$$

which, in further, is usually taken as

$$\omega^{D}(r) = [\omega^{R}(r)]^2 = \begin{cases} (1 - \frac{r_{ij}}{r_c})^2 & r_{ij} < r_c \\ 0 & r_{ij} \geqslant r_c \end{cases} \quad (7)$$

Finally, the spring force $\vec{f}^{S}$, which acts between the connected beads in a molecule, has the form of

$$\vec{f}_i^{S} = \sum_j C\vec{r}_{ij} \quad (8)$$

where C is a harmonic type spring constant for the connecting pairs of beads in a molecule, and is chosen equal to 4 (in terms of k_BT) [22].

Note that a modified version of the velocity-Verlet algorithm is used here to solve the Newtonian equation of motion [28]:

$$\begin{aligned} r_i(t+\Delta t) &= r_i(t) + v_i(t)\cdot\Delta t + \frac{1}{2}f_i(t)\cdot\Delta t^2 \\ \tilde{v}_i(t+\Delta t) &= v_i(t) + \lambda f_i(t)\cdot\Delta t \\ f_i(t+\Delta t) &= f_i[r_i(t+\Delta t),\ \tilde{v}_i(t+\Delta t)] \\ v_i(t+\Delta t) &= v_i(t) + \frac{1}{2}\Delta t\cdot[f_i(t) + f_i(t+\Delta t)] \end{aligned} \quad (9)$$

The parameter λ is introduced to account for some additional effects of the stochastic interactions. A detailed investigation of the effects of λ on the steady-state temperature has been reported by Groot and Warren [22]. For the particle density $\rho = 3$ and the constant $\sigma = 3$, they found an optimum value of $\lambda = 0.65$, in which the temperature control can be significantly maintained even at a large time step of 0.06. Here, we choose $\lambda = 0.65$ and the time step $\Delta t = 0.05$ according to Ref. [22].

The DPD simulations are performed in a cubic box of L^3 grids with periodic boundary conditions. The particle density ρ is set equal to 3. Hence, the total simulated DPD beads are $3L^3$. On the basis of the algorithm described above, the time evolutions of motion for these particles are started with an initially disordered configuration and simulated within the cubic box. Each simulation is performed until the formed structure remains somewhat unchanged with the time step. In general, the resulting morphology patterns via DPD are dependent of the finite size of the simulation box, as have been reported in other theoretical studies [29–31]. In order to exclude the finite size effects, one has to keep enlarging the simulation box size until the structures are no longer affected by the simulation box.

The dimensionless interaction parameter (i.e., in terms of k_BT) between like particles a_{II} when the particle density $\rho = 3$ is set equal to 25 according to the work of Groot and Warren [22]. The interaction parameter between different components I and J can be estimated by the following relationship between a_{IJ} and the Flory–Huggins interaction parameter χ_{IJ} derived by Groot and Warren [22] for $\rho = 3$,

$$a_{ij}(T) = a_{ii} + 3.497\chi_{ij}(T) \qquad i,j = A,B,C \quad (10)$$

Therefore, the value of $a_{ij} \leqslant 25$ corresponds to $\chi_{ij} \leqslant 0$, which indicates that components i and j are very miscible. As the incompatibility between i and j increases, a_{ij} increases from 25.

3. Self-assembling behavior of A-*block*-(B-*graft*-C) molecules

In simulating the phase behavior of A-*block*-(B-*graft*-C) copolymers by DPD, due to the fact that the interaction parameters a_{AB} and a_{BC} play a dominant role in the large-length-scale and small-length-scale of segregations, respectively, we let $a_{AC} = a_{BC}$ to reduce one interaction variable. Accordingly, here we aim to illustrate how the resulting morphology formation, in particular the experimentally observed structure-within-structure, is affected by a_{AB}, $a_{AC} = a_{BC}$, f_A, and the total degree of polymerization N.

Fig. 2 displays the phase diagram in terms of a_{AB} and $a_{BC} = a_{AC}$ for the systems with $f_A = 0.2$ and $N = 10$. We observe that in order to form the small-length-scale lamellar segregation between B and C within the large-scale BC-rich domains, not only the interaction parameters between B and C (a_{BC}) but also between the A-coil block and the BC-comb block (a_{AB} and a_{AC}) have to be significantly large. This can be illustrated clearly in Fig. 3, where $a_{AC} = a_{BC} = 70$. First, when the interaction parameters of a_{AC} and a_{BC} are large enough, both A and B components tend to segregate with C. However, if $a_{AB} \leqslant 25$, i.e., A and B are highly miscible, the microstructure formed by the system is mainly caused by the segregation between AB and C, and therefore, a stable segregated AB and C lamellar structure, $L_{AB,C}$, is observed for the system with comparable values of volume fractions of AB and C studied here. As a_{AB} increases, due to the fact that the immiscibility degree between A and B becomes more significant, the B component would gradually depart from the original AB-rich domains into the interfaces between A-rich and C-rich domains, and further stay in the C-rich domains. This behavior is analogous to decreasing the effective composition in the AB-rich domains, and thus a transition from $L_{AB,C} \rightarrow G_A \rightarrow C_A^{HEX} \rightarrow S_A$ occurs with an increase in a_{AB}. Furthermore, it is interesting to observe that when a_{AB} keeps increasing so that most of the B chains are pushed towards the C-rich domains, whereas, the fact that there also exists significant degree of incompatibility between B and C ($a_{AC} = a_{BC} = 70$) enables a small-length-scale B and C segregated lamellar phase formed within the large-length-scale BC-rich matrix.

To examine whether the DPD simulations can show the various types of structure-within-structures by varying the composition f_A, as have been frequently observed in experiments, we choose $a_{AC} = a_{BC} = 70$ and $a_{AB} = 100$. Fig. 4 displays the DPD simulation results at various values of f_A when $N = 20$. Generally speaking, with increasing the A composition f_A, the formed large-length-scale

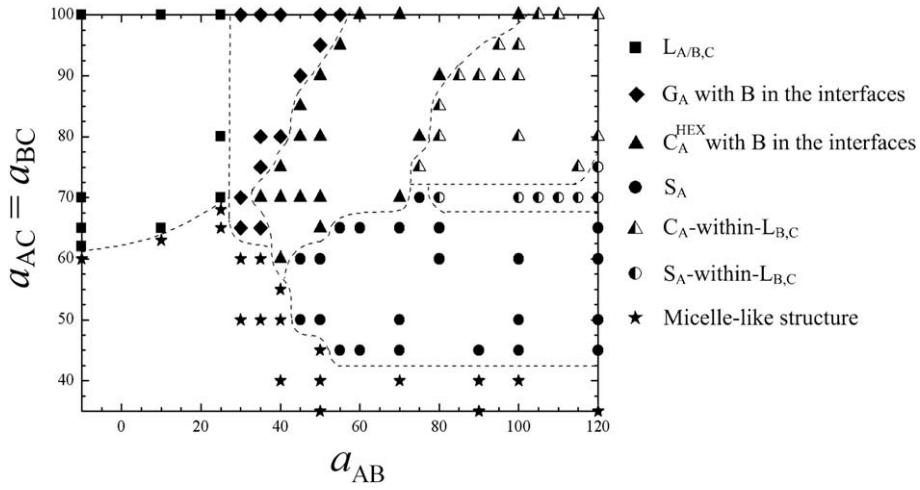

Fig. 2. Phase diagram of A-*block*-(B-*graft*-C) molecules with $f_A = 0.2$ and $N = 10$ in terms of the interaction parameter a_{AB} and $a_{BC} = a_{AC}$. The phase boundary lines are drawn to guide for the eyes.

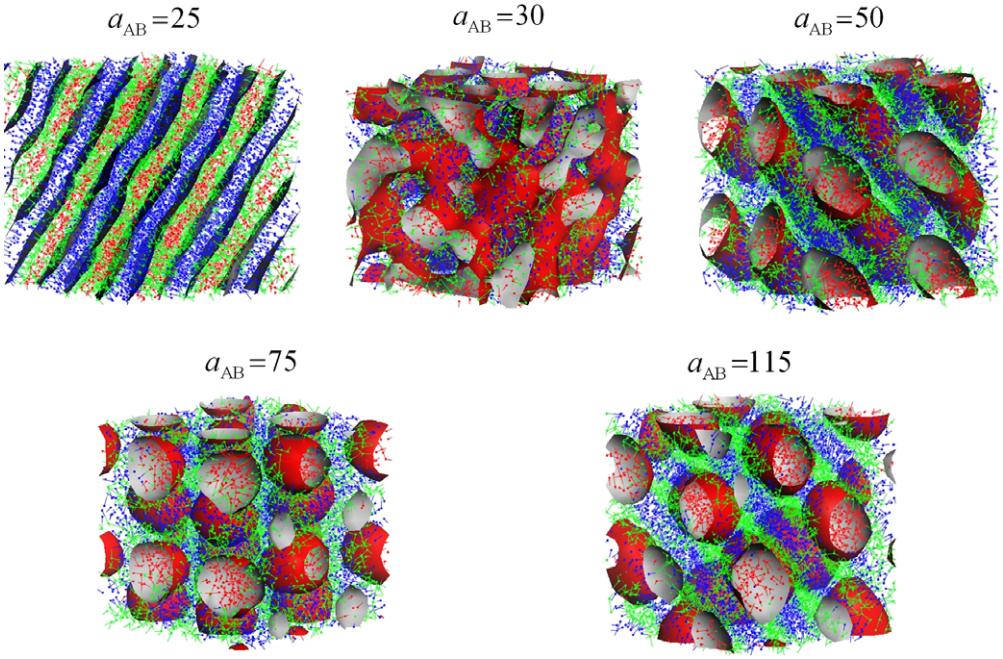

Fig. 3. Morphology variation of A-*block*-(B-*graft*-C) molecules with a_{AB} when $N = 10$, $f_A = 0.2$, and $a_{AC} = a_{BC} = 70$, simulated in a box size of $15 \times 15 \times 15$. The red, green, and blue colors represent A, B, and C, respectively. The red and blue surfaces correspond to the isosurfaces of component A and C, respectively. (For interpretation of the references to colour in this figure legend, the reader is referred to the web version of this article.)

morphology varies from $S_A \rightarrow C_A^{HEX} \rightarrow G_A \rightarrow L \rightarrow G_{BC} \rightarrow C_{BC}^{HEX} \rightarrow S_{BC}$, as expected. More interestingly, we observe that the formation of small-length-scale segregation between B and C within the BC-rich domains is dependent of f_A (more precisely, the length of the BC-comb block) at a fixed value of N. As can be seen in Fig. 4, when f_A is in the regime of 0.1–0.6 at $N = 20$, we have successfully simulated the following structure-within-structures: A-formed spheres in the matrix with B and C segregated lamellae (S_A-within-$L_{B,C}$), A-formed cylinders in the matrix with B and C segregated lamellae (C_A^{HEX}-within-$L_{B,C}$), and segregated B and C lamellae within the A-rich and BC-rich lamellae ($L_{B,C}$-within-$L_{A,BC}$). While, when $f_A \geqq 0.7$, we only observe that the B component stays in the interface between A-rich and C-rich domains. Indeed, this is reasonable due to the fact that when the length of the BC-comb block becomes short, the segregation degree between B and C is not significant enough to make these B and C well aligned to form lamellae. Hence, the resulting morphology is mainly driven by the segregation between A and C, and B acts more like a component in the interfaces. By increasing the length of the BC-comb block, one may expect that B and C will separate evidently and form a lamellar structure. For example, when f_A increases to 0.7 and 0.8, the total chain length N has to increase to 30 and 50, respectively, to ensure the formation of B and C lamellae within the BC-formed bicontinuous structures, as shown in Fig. 5. As f_A increases to 0.9, due to the fact that the BC-comb block is a very minor component, even though N increases to 60, we only observe the formation of A-spheres in the C-matrix.

4. Self-assembling behavior of A_2-*star*-(B-*alt*-C) Molecules

In examining the microphase separation behavior of A_2-*star*-(B-*alt*-C) copolymers, the DPD simulations are performed in a 3-D lat-

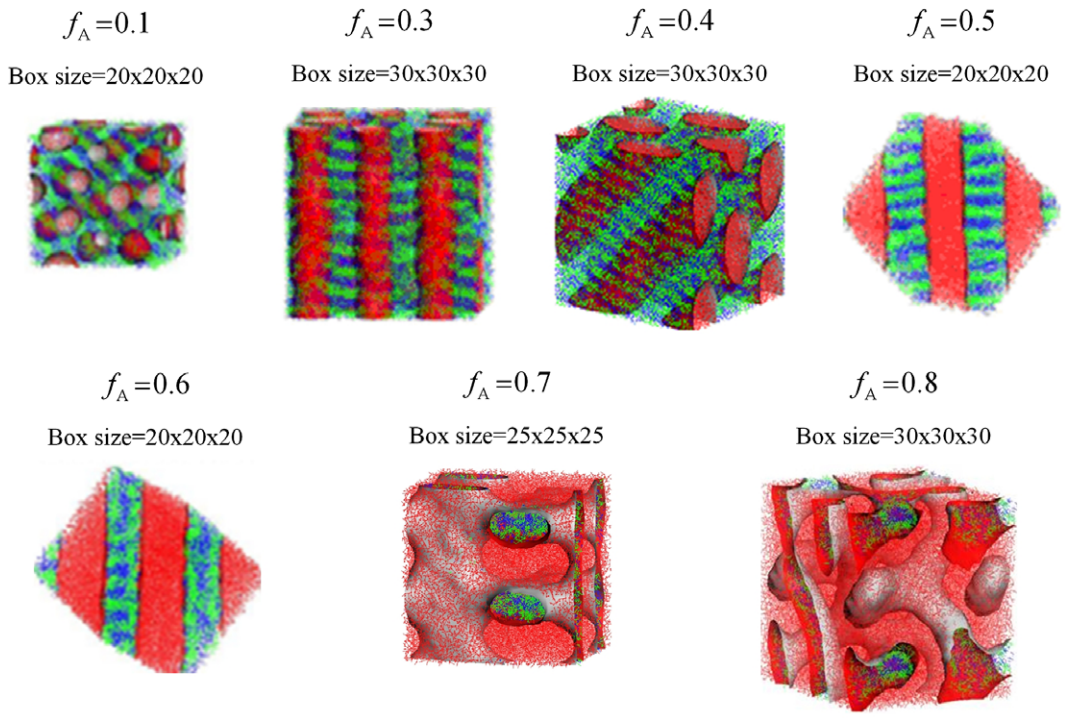

Fig. 4. Morphology variation of A-*block*-(B-*graft*-C) molecules with f_A when $N = 20$, $a_{AC} = a_{BC} = 70$, and $a_{AB} = 100$. The red, green, and blue colors represent A, B, and C, respectively. The red surface corresponds to the isosurface of component A. (For interpretation of the references to colour in this figure legend, the reader is referred to the web version of this article.)

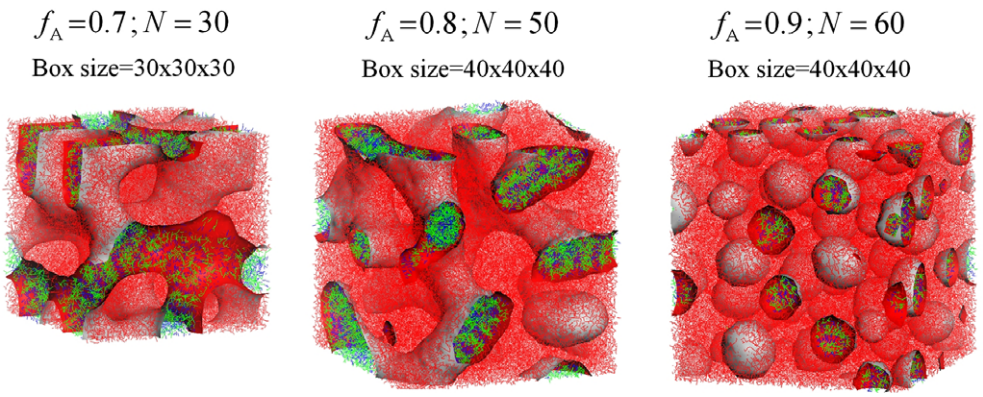

Fig. 5. Morphology patterns of A-*block*-(B-*graft*-C) molecules simulated at $a_{AC} = a_{BC} = 70$ and $a_{AB} = 100$ when $f_A \geqq 0.7$ and $N \geqq 30$. The red, green, and blue colors represent A, B, and C, respectively. The red surface corresponds to the isosurface of component A. (For interpretation of the references to colour in this figure legend, the reader is referred to the web version of this article.)

tice of size $20 \times 20 \times 20$ grids with periodic boundary conditions. This box size is chosen to ensure that the formed microstructures for our model copolymer with the total number of beads per chain $N = 13$ are no longer affected by the simulation box. In each simulated morphology pattern, the red, green and blue colors are used to represent A, B, and C, respectively. Among the interaction parameters between each pair of components I and J, a_{IJ}, I, J = A, B, C, due to the fact that the interaction parameters between the A-coil block and the BC-alternating block, i.e., a_{AB} and a_{AC}, play a dominant role in the large-length-scale diblock-like segregation; whereas a_{BC} drives the small-length-scale-ordering, we let $a_{AB} = a_{AC}$ to reduce one interaction variable.

First, the effects of the interaction parameters on the resulting structure patterns are illustrated in Fig. 6, where we construct the phase diagram in terms of a_{BC} and $a_{AB} = a_{AC}$ for the systems with $f_A = 0.54$. Similar to the previously introduced copolymers of A-*block*-(B-*graft*-C), all the three interaction parameters have to be large enough to ensure the formation of hierarchical structure-within-structures. To clarify, not only the interaction parameter between B and C but also the interaction parameters between the A-coil block and the BC-alternating block, i.e., a_{AB} and a_{AC}, has a great influence on the formation of small-length-scale B and C layers. When $a_{AB} = a_{AC}$ is large enough, i.e., the immiscibility degree between the A-coil block and the BC-alternating block becomes significant, the copolymers pack into an ordered A-rich and BC-rich segregated microstructure. Moreover, various diblock-like morphologies are induced by varying the interaction parameter a_{BC}. For instance, Fig. 7 illustrates a series of the morphology variation with a_{BC}, S_{BC} ($a_{BC} = -20$) $\rightarrow C^{HEX}_{BC}$ ($-10 \leqslant a_{BC} \leqslant 0$) $\rightarrow G_{BC}$ ($15 \leqslant a_{BC} \leqslant 25$) $\rightarrow L_{A,BC}$ ($30 \leqslant a_{BC} \leqslant 90$) $\rightarrow L_{B,C}$-within-$L_{A,BC}$ ($100 \leqslant a_{BC} \leqslant 120$), at $a_{AB} = a_{AC} = 100$. When a_{BC} is set to be 25, both B and C are indeed indistinguishable for A since $a_{AB} = a_{AC}$

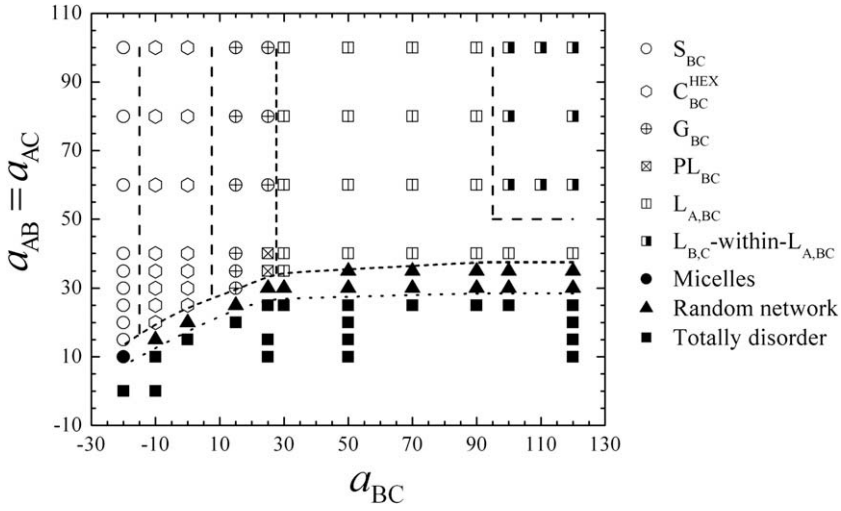

Fig. 6. Phase diagram of A_2-*star*-(B-*alt*-C) copolymers in terms of the interaction parameter $a_{AB} = a_{AC}$ and a_{BC} when $f_A = 0.54$ and $N = 13$. The phase boundary lines are drawn to guide for the eyes.

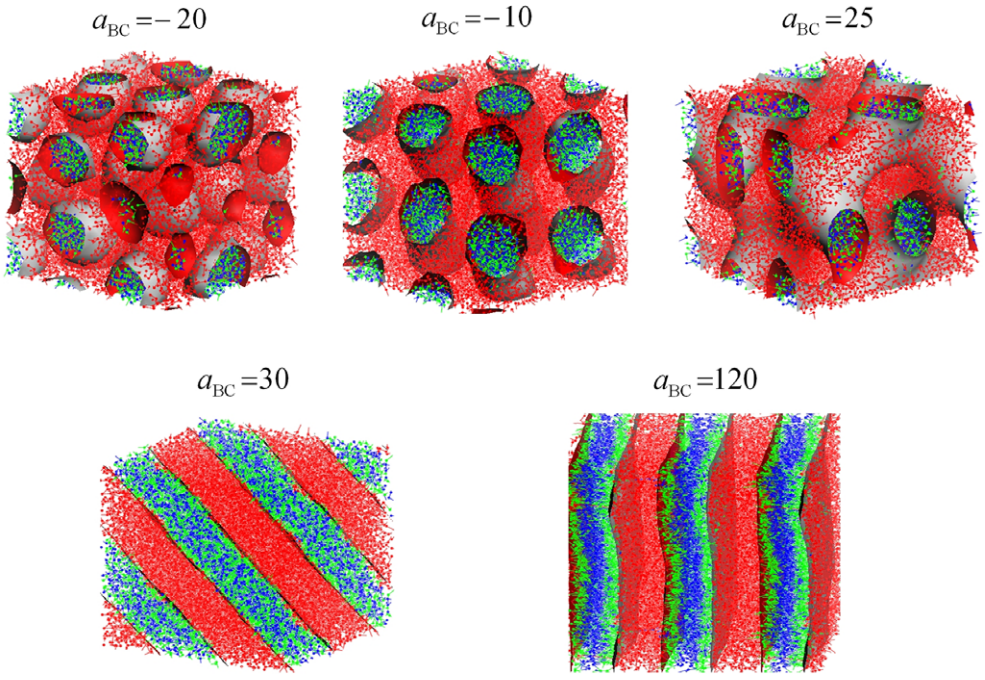

Fig. 7. Morphology variation of A_2-*star*-(B-*alt*-C) copolymers with a_{BC} when $f_A = 0.54$, $N = 13$, and $a_{AB} = a_{AC} = 100$, simulated in a box size of $20 \times 20 \times 20$. The red, green, and blue colors represent A, B, and C, respectively. The red surface corresponds to the isosurface of component A. (For interpretation of the references to colour in this figure legend, the reader is referred to the web version of this article.)

and the A_2-*star*-(B-*alt*-C) copolymers are identical to the so-called A_2B miktoarm star copolymers. Accordingly, the copolymer with $f_A = 0.54$ forms a complex gyroid phase G_{BC}, as have been predicted by self-consistent mean-field theory and simulated by DPD. When a_{BC} decreases from 25, due to the fact that B and C components become more attractive, the BC-alternating blocks tend to coil and transform into cylinders, and even spheres in the matrix of A-coil blocks. This transition behavior by decreasing a_{BC} is analogous to decreasing the composition of BC-alternating block. On the contrary, when a_{BC} increases from 25, though the segregation degree between B and C becomes more obvious, the systems still retain at a stable A-rich and BC-rich lamellar phase in a wide range of a_{BC} between 30 and 90, and no further di-block-like large-length-scale transition as mentioned above occurs. Indeed, these results are not surprising since when a_{BC} keeps increasing such that in order to reduce the contacts between B and C, the BC-alternating chain would rather fold within the original BC-rich layers to form small-length-scale B-rich and C-rich lamellae, i.e., the so-called hierarchical $L_{B,C}$-within-$L_{A,BC}$. Moreover, the resulting hierarchical periodicity is formed in parallel direction to each other, which is different from that in comb-coil copolymers. When the value of $a_{AB} = a_{AC}$ is fixed to a lower value such as 40, similar morphology transition associated with the large-length-scale-ordering has also been observed by varying the interaction parameter a_{BC}. Whereas, even when a_{BC} increases to a very large value of 120, we do not find the formation of the

hierarchical structure-within-structure morphology induced by a_{BC}, as in the case of $a_{AB} = a_{AC}$ at larger values. This manifests the fact that in order to form the small-length-scale lamellar segregation between B and C within the large-scale BC-rich domains, not only the interaction parameters between B and C (a_{BC}) but also between the A-coil block and the BC-alternating block (a_{AB} and a_{AC}) have to be significantly large.

To illustrate the various types of the structure-within-structures, which can be formed by A_2-*star*-(B-*alt*-C) copolymers in a wide range of composition f_A, we fix the values of $a_{AB} = a_{AC}$ at 100 and $a_{BC} = 120$. Fig. 8 displays the simulated structure-within-structures by varying f_A, such as A-formed spheres in the matrix formed by B and C alternating layers (S_A-within-$L_{B,C}$) ($f_A \cong 0.23$), hexagonally packed A-formed cylinders in the matrix with B and C segregated layers (C_A^{HEX}-within-$L_{B,C}$) ($f_A \cong 0.23$), $L_{B,C}$-within-$L_{A,BC}$ ($0.3 \leqslant f_A \leqslant 0.6$), coaxial B and C alternating domains within hexagonally packed BC-formed cylinders in the A-matrix ($L_{B,C}$-within-C_{BC}^{HEX}) ($0.65 \leqslant f_A \leqslant 0.7$), and cocentric BC-alternating domains within BC-formed spheres in the A-matrix ($L_{B,C}$-within-$S_{B,C}$) ($0.75 \leqslant f_A \leqslant 0.85$). Generally speaking, the geometry of large-length-scale morphology is mainly dominated by the composition f_A. If we further examine the small-length-scale formation of B and C alternating layers within the major domains, such as C_A^{HEX}-within-$L_{B,C}$ and $L_{B,C}$-within-$L_{A,BC}$, it is clear that these layers are parallel to the A-formed cylinders or lamellae. More interestingly, when f_A is larger than 0.5 so that B and C segregation occurs within the minor domains such as C_{BC}^{HEX} and S_{BC}, these BC-alternating chains fold in a particular way to form multiple (more than 2) B and C coaxial cylinders or cocentric spheres. These multiple coaxial cylinders or cocentric spheres formed by the BC-alternating blocks in the A_2-*star*-(B-*alt*-C) copolymers are possibly reported for the first time. Though it has been shown that the ABC linear triblock copolymers can form core-shell types of cylinders or spheres, the number of segregated layers within the domains is generally two instead of the multiple (more than two) layers that the A_2-*star*-(B-*alt*-C) can form.

When comparing the molecular alignment between these two systems of A-*block*-(B-*graft*-C) and A_2-*star*-(B-*alt*-C) in the structure-within-structures, as schematically plotted in Fig. 9, we observe a completely different packing behavior of molecules due to the difference of molecular architecture. Hence, the hierarchical structure-within-structures that these two copolymers can form are significantly different. In particular, the small-length-scale lamellae formed by the B-*alt*-C and B-*graft*-C chains display a parallel and perpendicular direction, respectively, with respect to the large-length-scale structure. We believe this characteristic difference could impose different influences upon various properties of polymers, such as photoelectronic properties, and lead to different potential applications.

Finally, in the coil-alternating copolymer system we would like to address that though the hierarchical structure type is maintained when the copolymer chain length increases, the number of small-length-scale lamellae that can form within the large-length-scale structure increases, as shown in Fig. 10. This is not surprising since when N increases, more B and C segments (beads) per chain can distribute freely, and hence more sublayers within the large-length-scale lamellae are possible. Recall that ten Brinke and co-workers [20] claimed that the number of internal layers within the lamellar-in-lamellar structure formed by the same types of copolymers in the strong segregation limit is mainly dominated by the balance between the stretching of the individual blocks and the interfacial area. In our DPD simulations, since we only use one bead to resemble each alternating block, the stretching effects associated with the entropy and flexibility of chains can

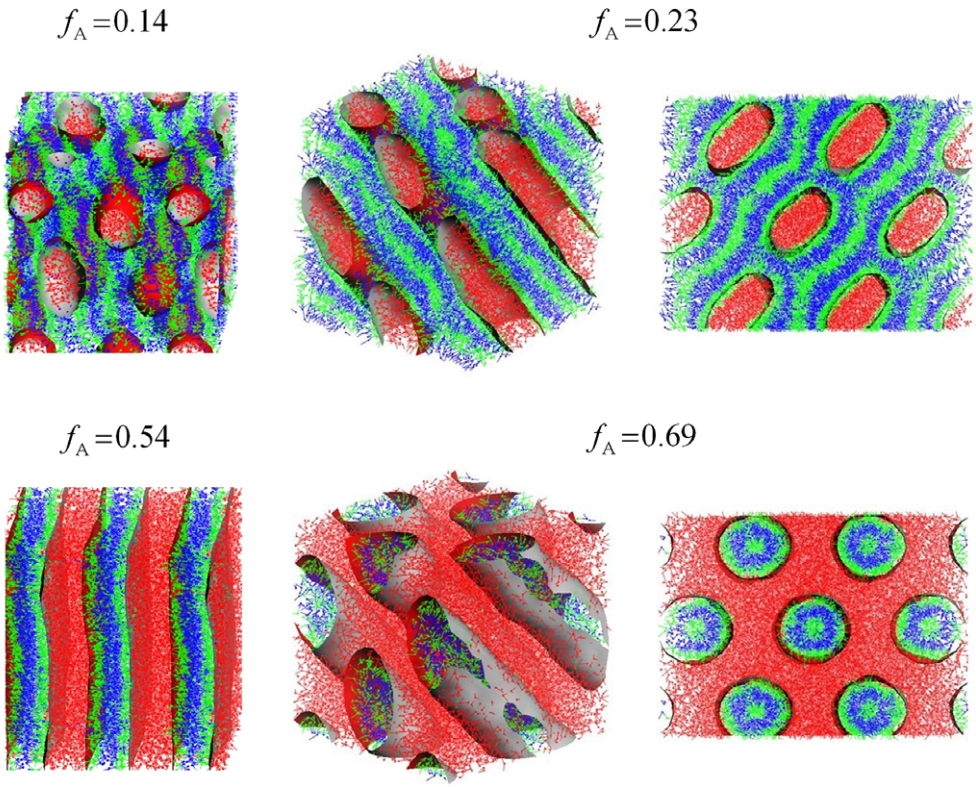

Fig. 8. Morphology variation of A_2-*star*-(B-*alt*-C) copolymers (N =13) with f_A when $a_{AB} = a_{AC} = 100$ and $a_{BC} = 120$, simulated in a box size of $20 \times 20 \times 20$. Note that the pattern when $f_A = 0.14$ corresponds to $N = 21$. The red, green, and blue colors represent A, B, and C, respectively. The red surface corresponds to the isosurface of component A. (For interpretation of the references to colour in this figure legend, the reader is referred to the web version of this article.)

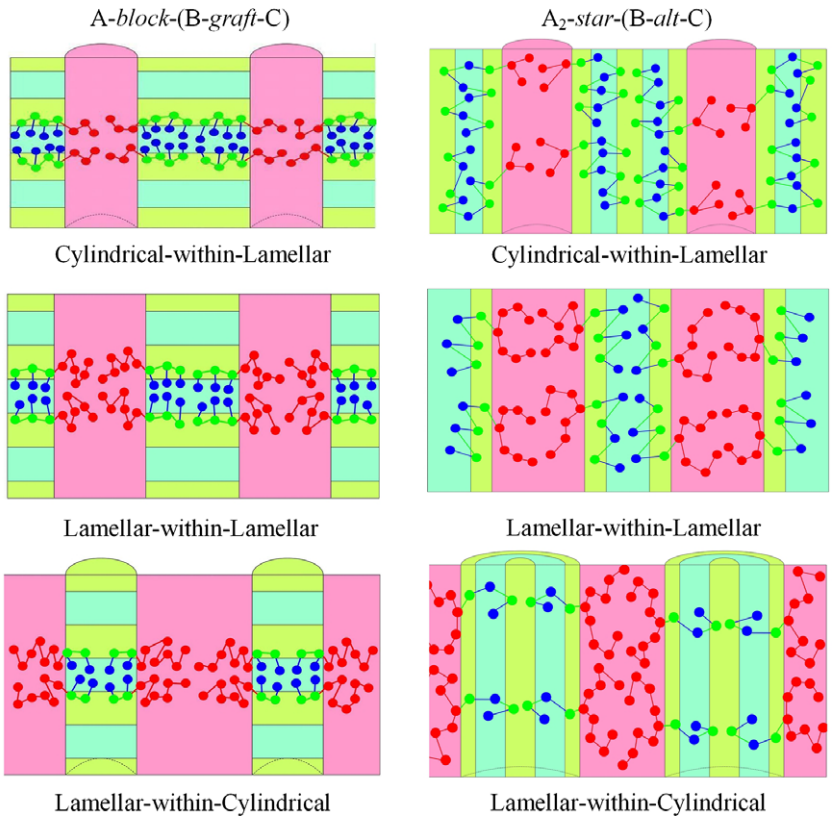

Fig. 9. Schematic plot of molecular arrangements for A-*block*-(B-*graft*-C) comb-coil and A_2-*star*-(B-*alt*-C) copolymers in various types of structure-within-structures.

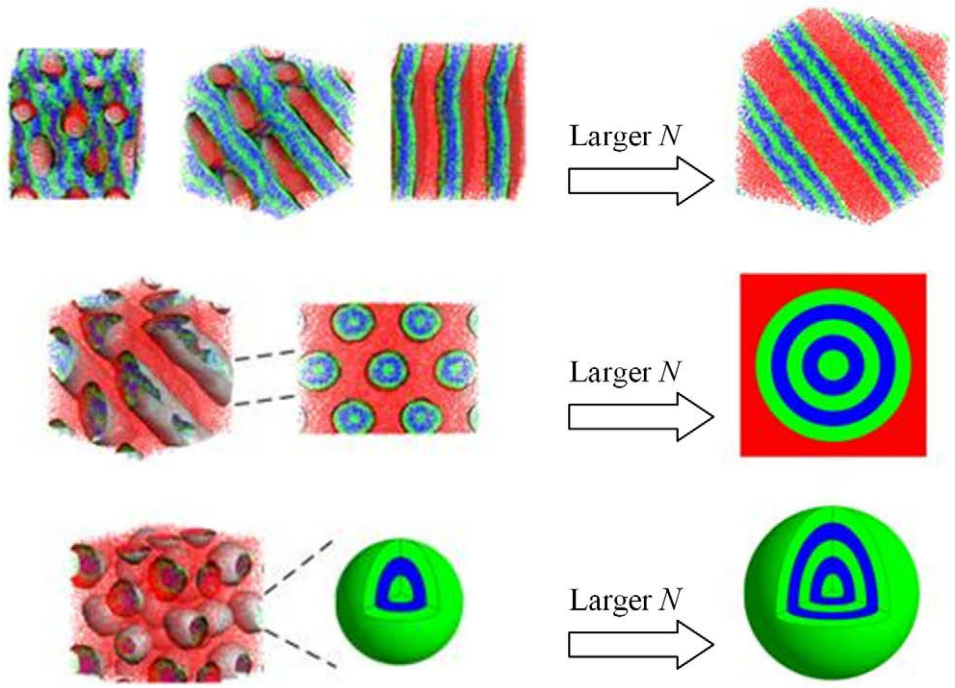

Fig. 10. Effect of increasing the total chain length on the formation of structure-within-structures in the A_2-*star*-(B-*alt*-C) copolymers.

not be treated properly. Still, the fact that each bond between two connected beads in our model is flexible enables the chains with more B and C alternating segments to create more possible distribution ways and hence to form more internal-layered structures.

5. Conclusion

Copolymers with hierarchical structures have gained increasing degrees of interest and attention both in fundamental and applied fields of polymer science. Two typical molecular architectures of

coil-comb and coil-alternating block copolymers have been shown good candidates to form hierarchical structure-within-structures by experiments. Theoretically, we employ a direct simulation method of the dissipative particle dynamics (DPD) to examine the self-assembling behavior of A-*block*-(B-*graft*-C)) and A_2-*star*-(B-*alt*-C) molecules. As long as the three components are significantly incompatible one another, we have successfully simulated various types of hierarchical structure-within-structures in both copolymer architectures, as have been reported in experimental studies. However, they exhibit a completely different packing behavior of molecules due to the difference of molecular architecture. In particular, the small-length-scale lamellae formed by the B-*alt*-C and B-*graft*-C chains display a parallel and perpendicular direction, respectively, with respect to the large-length-scale structure.

In addition to the block composition, varying the interaction parameters can also induce a series of morphology transitions associated with two-length-scales. Moreover, the chain length is observed to impose different effects on the formation of hierarchical structure-within-structures in these two molecular architectures. In the A-*block*-(B-*graft*-C) copolymer melts, when the chain length is small, since the length of the BC-comb block is not long enough to ensure the formation of well ordered B and C lamellar segregation, the resulting morphology is mainly in the large-length-scale ordering with most of the B segregated along the interfaces between the A-rich and C-rich domains. By increasing the length of the BC-comb block, both B and C can pack orderly to form a lamellar structure, and thus various structure-within-structures are formed. In the A_2-*star*-(B-*alt*-C) copolymer melts, when the chain length increases, it is reasonable to infer that the flexible copolymer chains with more alternating B and C blocks can create more possible folded ways within the large-length-scale domains. Hence, the number of B and C alternating segregated layers that can form within the large-length-scale structure increases.

Acknowledgments

This work was supported by the National Science Council of the Republic of China through Grant NSC 96-2221-E-002-019.

References

[1] N. Hadjichristidis, S. Pispas, G. Floudas, Block Copolymers: Synthetic Strategies, Physical Properties, and Applications, Wiley, New Jersey, 2003.
[2] M.W. Edens, R.H. Whitmarsh, I.W. Hamley, Developments in Block Copolymer Science and Technology, Wiley, New York, 2004.
[3] J. Ruokolainen, R. Makinen, M. Torkkeli, T. Makela, R. Serimaa, G. Serimaa, O. Ikkala, Science 280 (1998) 557.
[4] J. Ruokolainen, G. Ten Brinke, O. Ikkala, Adv. Mater. 11 (1999) 777.
[5] J. Ruokolainen, M. Saariaho, O. Ikkala, G. ten Brinke, E. Thomas, M. Torkkeli, R. Serimaa, Macromolecules 32 (1999) 1152.
[6] R. Maki-Ontto, K. de Moel, E. Polushkin, G.A. van Ekenstein, G. ten Brinke, O. Ikkala, Adv. Mater. 14 (2002) 357.
[7] O. Ikkala, G. ten Brinke, O. Ikkala, Chem. Commun. (2004) 2131.
[8] G. ten Brinke, O. Ikkala, The Chemical Record 4 (2004) 219.
[9] E. Polushkin, S. Bondzic, J. de Wit, G. Alberda van Ekenstein, I. Dolbnya, W. Bras, O. Ikkala, G. ten Brinke, Macromolecules 38 (2005) 1804.
[10] A. Laiho, R.H.A. Ras, S. Valkama, J. Ruokolainen, R. Osterbacka, O. Ikkala, Macromolecules 39 (2006) 7648.
[11] W. van Zoelen, G. Alberda van Ekenstein, O. Ikkala, G. ten Brinke, Macromolecules 39 (2006) 6574.
[12] S. Valkama, T. Ruotsalainen, A. Nykanen, A. Laiho, H. Kosonen, G. ten Brinke, O. Ikkala, J. Ruokolainen, Macromolecules 39 (2006) 9327.
[13] C.S. Tsao, H.L. Chen, Macromolecules 37 (2004) 8984.
[14] Y. Nagata, J. Masuda, A. Noro, D. Cho, A. Takano, Y. Matsushita, Macromolecules 38 (2005) 10220.
[15] J. Masuda, A. Takano, Y. Nagata, A. Noro, Y. Matsushita, Phys. Rev. Lett. 97 (2006) 098301.
[16] J. Masuda, A. Takano, J. Suzuki, Y. Nagata, A. Noro, K. Hayashida, Y. Matsushita, Macromolecules 40 (2007) 4023.
[17] R.J. Nap, C. Kok, G. ten Brinke, S.I. Kuchanov, Eur. Phys. J. E 4 (2001) 515.
[18] R.J. Nap, G. ten Brinke, Macromolecules 35 (2002) 952.
[19] R. Nap, I. Erukhimovich, G. ten Brinke, Macromolecules 37 (2004) 4296.
[20] R. Nap, N. Sushko, I. Erukhimovich, G. ten Brinke, Macromolecules 39 (2006) 6765.
[21] P. Hoogerbrugge, J. Koelman, Eur. Phys. Lett. 19 (1992) 155.
[22] R.D. Groot, P.B. Warren, J. Chem. Phys. 107 (1997) 4423.
[23] C.I. Huang, Y.C. Lin, Macro. Rapid Commun. 28 (2007) 1634.
[24] C.I. Huang, C.M. Chen, Chem. Phys. Chem. 8 (2007) 2588.
[25] M.W. Matsen, F.S. Bates, Macromolecules 29 (1996) 1091.
[26] G.M. Grason, R.D. Kamien, Macromolecules 37 (2004) 7371.
[27] P. Espanol, P.B. Warren, Eur. Phys. Lett. 30 (1995) 191.
[28] M.P. Allen, D.J. Tildesley, Computer Simulation of Liquids, Clarendon, Oxford, 1987.
[29] U. Micka, K. Binder, Macromol. Theory Simul. 4 (1995) 419.
[30] Y. Bahbot-Raviv, Z.G. Wang, Phys. Rev. Lett. 85 (2000) 3428.
[31] Q. Wang, P.F. Nealey, J.J. de Pablo, Macromolecules 34 (2001) 3458.